

Instruction-Guided Scene Text Recognition

Yongkun Du, Zhineng Chen, *Member, IEEE*, Yuchen Su, Caiyan Jia, and Yu-Gang Jiang, *Fellow, IEEE*

Abstract—Multi-modal models show appealing performance in visual recognition tasks recently, as free-form text-guided training evokes the ability to understand fine-grained visual content. However, current models are either inefficient or cannot be trivially upgraded to scene text recognition (STR) due to the composition difference between natural and text images. We propose a novel instruction-guided scene text recognition (IGTR) paradigm that formulates STR as an instruction learning problem and understands text images by predicting character attributes, e.g., character frequency, position, etc. IGTR first devises *(condition, question, answer)* instruction triplets, providing rich and diverse descriptions of character attributes. To effectively learn these attributes through question-answering, IGTR develops lightweight instruction encoder, cross-modal feature fusion module and multi-task answer head, which guides nuanced text image understanding. Furthermore, IGTR realizes different recognition pipelines simply by using different instructions, enabling a character-understanding-based text reasoning paradigm that considerably differs from current methods. Experiments on English and Chinese benchmarks show that IGTR outperforms existing models by significant margins, while maintaining a small model size and efficient inference speed. Moreover, by adjusting the sampling of instructions, IGTR offers an elegant way to tackle the recognition of both rarely appearing and morphologically similar characters, which were previous challenges. Code: <https://github.com/Topdu/OpenOCR>.

Index Terms—Scene text recognition, instruction learning, multi-modal learning, character attribute.



1 INTRODUCTION

SCENE text recognition (STR) is a longstanding pattern recognition task that focuses on reading natural text images. Essentially, STR is a multi-modal task that learns a mapping from image modality to text modality, aiming to decipher the character sequence. Over the past years, a magnitude of methods have been devoted to STR and different recognition pipelines like parallel recognition (PR) [1]–[7] and auto-regressive recognition (AR) [8]–[11] have been developed, which satisfy the diverse accuracy and speed needs in various applications.

Recently, there is a trend to develop multi-modal models [12]–[15] for the generic visual recognition tasks [16], [17]. Notably, pioneering models such as Grounding-DINO [13] and SAM [14] have embraced the integration of natural language as instructive guidance, which enables a profound understanding of fine-grained visual content. For instance, by using free-form text rather than categorical labels for training [13], the learned model is capable of understanding more specific objects like *the left lion* rather than *lion*, and meanwhile, resulting in superior performance compared to uni-modal models in typical benchmarks [18], [19].

Similarly, STR models could benefit significantly from an enhanced ability to understand text images thoroughly. However, given the distinct compositional elements of nat-

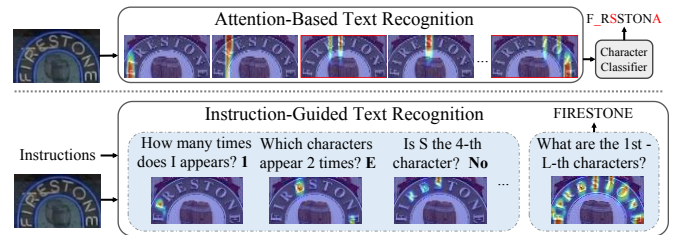


Fig. 1. **Upper**: popular attention-based STR models follow the pipeline of positioning visual features for every character and then classifying. Misrecognitions may happen if features are positioned incorrectly. **Bottom**: IGTR comprehends the text image first and then recognition. It understands the question and associates its answer with the corresponding visual features, generating robust instruction-guided STR.

ural and text images, achieving this presents considerable challenges when trivially applying existing instruction learning schemes [13], [14], [20]–[22] to STR. Unlike natural images, which can depict objects and scenes from the physical world and be effectively described using natural language, the text image is typically described by a single word. When the word is simply treated as language, it provides limited semantic context to guide the STR model understanding the text image. Therefore, developing rich instructional strategies for STR tasks is an urgent necessity. Moreover, the text image is composed of sequentially arranged characters, necessitating the exploration of character-central properties to facilitate a deep understanding of the text. However, how to explore these properties and how they benefit text recognition are less studied in existing solutions. Furthermore, with the popularity of using OCR models in mobile and edge scenarios, where lightweight STR models [1], [5], [23] are required, it is yet to explore further multi-modal STR models that run fast and are less demanding in computational resources.

This work was supported by the National Key R&D Program of China (2022YFB3104703), and in part by the National Natural Science Foundation of China (32341012).

- Yongkun Du, Zhineng Chen, Yuchen Su and Yu-Gang Jiang are with the School of Computer Science, Fudan University, Shanghai 200433, China. E-mail: {ykdu23, ycsu23}@m.fudan.edu.cn, {zhinchen, ygj}@fudan.edu.cn.
- Caiyan Jia is with the School of Computer and Information Technology, Beijing Jiaotong University, Beijing 100044, China. E-mail: cjia@bjtu.edu.cn.

Corresponding author: Zhineng Chen.

TABLE 1

Character attribute prediction instructions (taking *ARTETA* as the example), where **red** in *Question* column denotes character or numerical variables. Different colors in *Type* column represent different types of questions. Character is abbreviated to char. The same below.

Condition	Condition Option	Question	Answer	Type
1. Char $\{c_i\}$ in the image 2. Char $\{c_i\}$ appear $\{N_i\}$ times 3. The i -th char are c_i 4. Sub-string $\{c_s - c_{s+m}\}$ in the image 5. There are L chars in the image 6. None	1/2/3/4/5/6	How many A in the image?	2	Frequency
	1/2/3/4/5/6	How many A in the first 3 chars?	1	Constrained frequency
	1/2/3/4/5/6	Does A appear 2/1 times in the image?	Yes/No	Status
	1/2/3/4/5/6	Does A appear 2/1 times in the first 3 chars?	No/Yes	Constrained status
	1/2/3/4/5/6	Which char in the image is E ?	4-th	Position
	1/2/3/4/5/6	Is A the 1st/5 -th char in the image?	Yes/No	Search status
	1/2/3/4/5/6	Which chars appear 2 times?	A and T	Char
	1/2/3/4/5/6	Which chars appear 1 time in first 3 chars?	A, R and E	Constrained char
	1/2/3/4/5/6	Where is the sub-string RTE/RTS ?	2nd/None	Sub-string position
	1/2/3/4/5/6	Is sub-string RTE at position 2/3 ?	Yes/No	Sub-string status
1/2/3/4/6	How many chars in the image?	6	Length frequency	
5/6	What are the first and last chars?	A/A	Edge char	

TABLE 2

Text recognition instructions, where each row simulates a different recognition pipeline.

Condition	Question	Answer	Type
None	What are the 1st to L-th chars in the image?	$c_1 - c_L$	Parallel recognition
1st to i -th chars are $c_1 - c_i$	What is the $i+1$ -th char?	c_{i+1}	Auto-regressive recognition
1st to $i-1$ -th, $i+1$ -th to j -th chars are known	What is the i -th char?	c_i	Re-identification
There is a sub-string $c_i - c_j$	What is the previous/next char of the sub-string?	c_{i-1}/c_{j+1}	Extrapolating recognition

In this paper, we aim to build an efficient instruction-learning-based paradigm for STR. Our proposed method, termed instruction-guided STR (IGTR), has made meaningful attempts in both instruction construction and learning architecture design. For instruction construction, to evoke a human-like understanding and recognition of the text image, we first define character attributes as a set of statuses regarding the status, position, and frequency of character or character combinations within a text. Then, we construct two types of instructions tailored to character attribute prediction and text recognition, respectively. Specifically, we argue that character attributes are critical components to establishing a deep understanding of the text. As a result, rich and diverse character attribute prediction instructions in the form of $\langle \text{condition}, \text{question}, \text{answer} \rangle$ are devised, where *condition* denotes attributes already known, and *question-answer* is question-answer pair regarding learning the rest attributes, as shown in Tab. 1. Meanwhile, recognition instructions of the same form are proposed to simulate different text recognition pipelines, including PR, AR and other useful but less-explored ones. Each can be realized simply by using one of the instructions, as shown in Tab. 2.

With the instructions, we develop a dedicated learning architecture for both attribute prediction and text recognition. It consists of an instruction encoder to generate textual embeddings based on instructions, a cross-modal feature fusion module for characterizing interactions between image and text modalities, and a multi-task answer head responsible for answering different questions and reading the text. IGTR adopts a two-stage training process. First, it is pre-trained using a large number of attribute prediction instructions, which endows the model with a profound understanding of character attributes. Then, it is fine-tuned by recognition instructions, which enables the model’s superior text recognition capability. All attribute prediction instructions are sampled online during training and the

whole architecture enjoys an end-to-end optimization.

We conduct extensive experiments on English and Chinese benchmarks. The results show that IGTR has quite impressive performance. No matter following PR or AR pipeline, IGTR outperforms existing models by clear margins in terms of accuracy, while still maintaining a small model size and efficient inference speed. Meanwhile, the attribute prediction instructions guide meaningful text understanding, even when solely pre-trained on them, the model exhibits impressive *zero-shot* recognition capability. In addition, IGTR enjoys remarkable learning flexibility inherited from its instruction-guided nature. By simply adjusting the rule of instruction sampling, IGTR exhibits superior performance in recognizing both rarely appearing and morphologically similar characters, which were common challenges for previous methods.

IGTR represents a novel paradigm of STR. As exemplified in Fig. 1, the top half represents the recognition pipeline of popular attention-based STR models. They utilize the attention mechanism to position visual features for every character and then use the features to perform character classification. Mis-recognitions may happen if features are positioned incorrectly. In contrast, as shown in the bottom half, IGTR successfully grasps character attributes and the text image by exhaustive question-answering-based learning. Therefore visual features make a correct response and IGTR generates more robust recognition. On the other hand, recent large multi-modal models such as LLaVA [21] and Monkeys [22], [24], trained or fine-tuned on OCR-relevant dialog datasets [25], also show remarkable performance in multiple OCR-related tasks including STR. However, these models typically have huge parameters and are highly demanding in computational resources. In contrast, the size of IGTR is 24.1M, and different IGTR models consume 4ms-10ms only when inferring a text instance in one NVIDIA 1080Ti GPU, both are appealing properties in mobile and

edge computing applications.

Contributions of this paper are summarized as follows.

- We propose IGTR that regards STR as a cross-modal instruction learning task. Unlike existing models, IGTR facilitates text recognition by comprehending text images, presenting a novel paradigm for STR.
- We introduce rich and diverse instruction triplets $\langle condition, question, answer \rangle$, and develop a dedicated architecture to effectively learn these instructions and the text image, establishing the first instruction-guided STR solution.
- Through extensive experiments, we demonstrate the effectiveness of IGTR not only in public benchmarks, but also in providing a uniform framework to tackle common STR challenges flexibly.

2 RELATED WORK

2.1 Scene Text Recognition (STR)

We can broadly classify existing sequence-based STR models into two types according to their recognition pipelines, i.e., PR and AR. PR identifies all the characters within the text image at once. It can be further classified as CTC-based and encoder-decoder-based parallel decoding ones. The former [1], [5], [26] assumes that the text image can be implicitly split into a series of stripes from left to right, each corresponding to a recognition unit, i.e., a character or blank. The recognized unit sequence is then optimized by the CTC rule [27] to get recognition results. The second [2], [3], [6], [7], [28], [29] commonly adopt an attention-based encoder-decoder framework. They first allocate a fixed number of placeholders, each corresponding to a character, and then learn how to fill in the placeholders with proper features and deduce the characters in parallel. These methods often have fast inference speed. However, early studies may not perform well when encountering text deformation. Recent studies propose various ways of utilizing language and other clues, for example, knowledge distillation [28], external language models [3], [7], [29], character counting [6], etc., which improve the recognition accuracy remarkably.

In contrast, AR [8]–[10], [30] adopts a one-by-one sequential recognition pipeline. It is introduced to STR following the success in NLP [31]. These models utilize previously decoded characters as language clues to assist recognition, thus getting better results in general. However, their inference speed is slow, and also may suffer from the problem of attention drift when encountering rarely seen text images like highly deformed text [32]. To mitigate attention drift, some methods [32]–[34] proposed to utilize the position clue. Meanwhile, permuted and bidirectional recognition are developed [11], [35], providing a stronger language prior. Generally, AR provides more natural and finer language integration compared to PR. However, only a few previously identified characters are incorporated as guidance, which limits the assistance from the language.

In addition to the two types above, there also are a few studies employing double-check techniques to assist recognition. For example, character re-identification has been considered in several methods [2], [3], [11], [36]. Typically, they use language models to correct initial results from PR or AR.

Despite improving the accuracy, however, miscorrections may also happen especially for contextless text.

2.2 Multi-Modal Visual Recognition

Multi-modal models [16], [17] has received widespread attention recently, especially in visual recognition tasks, as instruction learning can evoke an appealing ability to understand fine-grained visual content. CLIP [20] and ALIGN [37] are pioneering studies in this direction. They have performed cross-modal contrastive learning on billion-level image-text pairs, enabling impressive zero-shot image classification [19]. Later, GLIP [12] and Grounding-DINO [13] introduce instruction-based object detection [18]. They utilize instructions of free-form language for training, and can detect objects that exactly match the language. Similar approaches are explored in image segmentation, for instance, the well-regarded SAM [14] and SegGPT [15]. These models leverage rich interactive instructions such as clicks, boxes, masks and text to achieve generic and deep visual understanding, enabling segmentation of anything. Instruction-based recognition has also been applied to tasks like license plate recognition [38] and speech recognition [39]. However, they are more like applications of VQA models [40], [41] or generative models [42], [43] dedicated to these tasks.

Our study is also related to recent research efforts on large multi-modal models. One is prompt engineering on pre-trained visual-language models [44], which performs recognition based solely on prompts without updating model parameters. Typically, it uses an image and a text question to query the model and get the answer [45], [46], which can also reply STR-related questions. Another is large multi-modal models fine-tuned on OCR, for example, LLaVA [21] and Monkeys [22], [24]. They are capable of performing multiple OCR-related tasks like document understanding or key information extraction without relying on traditional OCR tools [23]. However, these models typically consume substantial resources in downstream applications, restricting their use in mobile and edge computing scenarios where lightweight STR models [1], [5], [23], [47] are adopted widely. To date, instruction-based STR is not well explored especially its efficient implementation.

3 METHOD

Our method consists of two parts, i.e., instruction construction and sampling, IGTR architecture and learning. The instructions, including both character attributes prediction and recognition ones, are $\langle condition, question, answer \rangle$ triplets. The triplet composition ensures that many instructions can be generated for attribute learning even for a short text, and meanwhile, different recognition pipelines can be precisely described. On the other hand, IGTR architecture is developed to enable efficient encoding of the instructions, and then effective cross-modal learning and recognition. They are detailed as follows.

3.1 Instruction Construction and Sampling

We mainly introduce character attribute prediction instructions here and recognition instructions will be outlined later. As shown in Tab. 1, a series of character attribute prediction

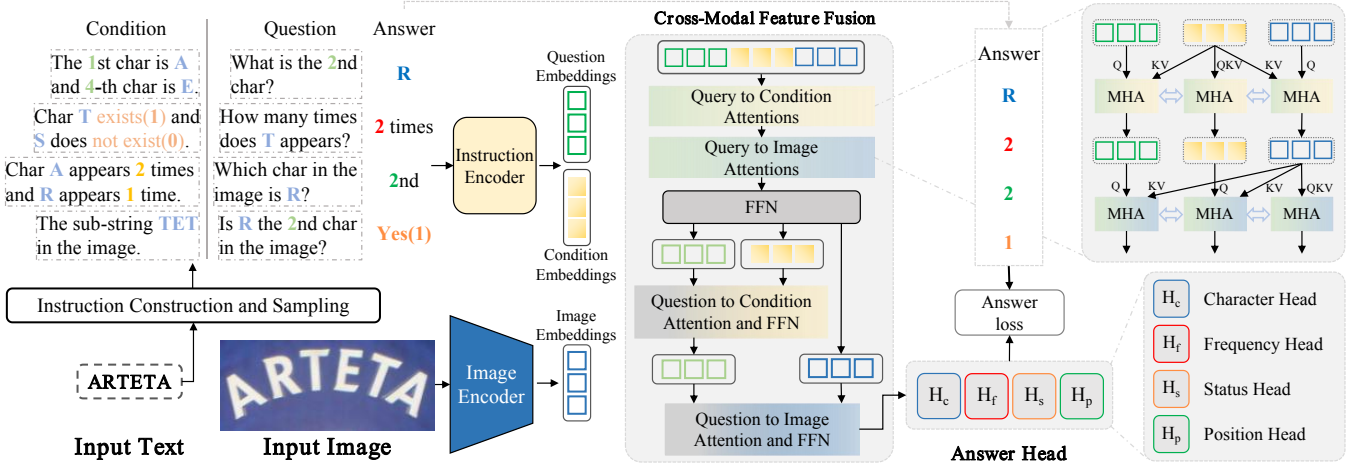


Fig. 2. Overview of Instruction-Guided STR. Instruction triplets $\langle condition, question, answer \rangle$ are sampled from text *ARTETA*, where *condition* and *question* are encoded as the corresponding embeddings by the instruction encoder. Meanwhile, the image embedding is extracted from the image encoder. The three embeddings are interacted and fused by the cross-modal feature fusion module, and a multi-task answer head is appended to answer different types of questions. The whole architecture enjoys a lightweight design and end-to-end optimization. Best viewed in color.

instructions are proposed. Each instruction consists of a *condition*, a *question*, and an *answer*. The *condition* means character attributes given in advance, and the *question-answer* pair corresponds to the specified query and its response.

We have meticulously crafted various instructions to ensure that the text and characters can be thoroughly described. As seen in Tab. 1, the questions can be grouped into four types according to their answers (highlighted by different colors), i.e., *char*, *frequency*, *position*, and *status*. These questions compel the model to assess the relevance of each character from different aspects, determining whether it contributes to the answer. This process, in turn, guides the model towards attribute understanding.

Given a text, we further define five types of character attributes: character-status (*cs*) represents whether a specific character exists, character-frequency (*cf*) denotes the occurrence times of a specific character, constrained character-frequency (*cf_{cons}*) describes character-frequency given a specific constraint (e.g., the first 3 characters), position-character (*pc*) means the character at the *i*-th position, and sub-string (*ss*) denotes a certain length sub-string. For example, given text *ARTETA*, assuming the constraint is the first 3 characters and the sub-string length *m* is set to 3, character attributes can be obtained by traversing the text, as expressed in the following set form:

$$\begin{aligned}
 cs &= [[A,1], [B,0], \dots, [E,1], \dots, [R,1], [S,0], [T,1], \dots, [Z,0]] \\
 cf &= [[A,2], [E,1], [R,1], [T,2]] \\
 cf_{cons=3} &= [[A,1], [E,0], [R,1], [T,1]] \\
 pc &= [[0,A], [1,R], [2,T], [3,E], [4,T], [5,A]] \\
 ss_{m=3} &= [[0, ART], [1, RTE], [2, TET], [3, ETA]]
 \end{aligned}$$

Note that each element in those sets is represented by a square bracket with two units, corresponding to the variables in question and answer, and shown in Tab. 1.

We propose to enlarge the traditional question-answer instruction to $\langle condition, question, answer \rangle$ triplet. Specifically, a partitioning strategy is proposed to split character attributes into two parts: one is *condition* to represent al-

ready known attributes, and the other is attributes left for question-answer-based model learning. Assuming that the *condition* is $[[E,1], [R,1], [S,0]]$, $[[E,1],[T,2]]$ and $[[0,A], [2,T], [5,A]]$, which are subsets of *ce*, *cf* and *pc*, respectively. The *condition* can be described as follows: “The characters *E* and *R* exist in the image, but *S* does not exist”; “The character *T* appears twice and *E* appears once in the image”; and “The 1st/3rd/6-th character in the image is *A/T/A*”. Take the set split on *pc* as an example, the remaining subset is $[[1,R], [3,E], [4,T]]$, allowing questions such as “Which character in the image is *R/E/T*?” with answers “the 2nd/4-th/5-th one” for model training. Other question-answer pairs are generated similarly. According to the types of answer, questions and answers are categorized into four types, i.e., $Ques = [Q_{c_i}, Q_{f_j}, Q_{p_r}, Q_{s_s}]$ and $Ans = [A_{c_i}, A_{f_j}, A_{p_r}, A_{s_s}]$, where the suffixes *c*, *f*, *p*, and *s* denote the answer type is *char*, *frequency*, *position*, and *status*, respectively.

The triplet form notably increases the richness and diversity of instructions. To sample instructions for each input text during model training, we repeat the partitioning strategy (*GenInsts*) *K* times, with the *condition* randomly shuffling and splitting each time to ensure disjoint and varied instructions. This process is carried out by `RandomSplit(Attributes)`, as described in Algorithm 1. For each partition, we enumerate all possible question-answer variables and up to $\sum_{p=1}^N (L-p) \frac{N!}{p!(N-p)!}$ different instructions could be sampled, where *N* is the number of attributes ($\text{len}(\text{atrb})$), *p* represents the number of attributes in *condition* and it is randomly obtained using `random.randint(len(atrb))`. Moreover, by sampling *K* times, we get a large number of instructions. Consequently, the instructions and text image constitute an overwhelming many-to-one correspondence, where the language modality has been significantly enriched.

3.2 IGTR Architecture and Learning

The IGTR architecture is depicted in Fig. 2. We also take *ARTETA* as the example for illustration. First, the sampled

Algorithm 1: Pseudo-code of instruction sampling and model optimization in IGTR

```

import random
# text, image from training dataset
# cs: character-status attribute set
# cf: character-frequency attribute set
# pc: position-character attribute set
# ss: sub-string attribute set
def RandomSplit(atrbs):
    Cond=[], QA=[]
    for atrb in atrbs:
        p = random.randint(len(atrb))
        random.shuffle(atrb)
        Cond.append(atrb[p:])
        QA.append(atrb[:p])
    return Cond, QA
def GenInsts(Attributes):
    Cons = random.randint(len(text))
    # Generating attributes for constraints
    cf_cons = GenConsCF(text, Cons)
    Attributes += [cf_cons]
    Cond, QA = RandomSplit(Attributes)
    # grouping QA into four types by answer
    Ques, Ans = GenQAbyType(QA, text)
    return Cond, Ques, Ans # instruction
Attributes = [cs, cf, pc, ss]
E_I = ImageEncoder(image)
LossSum = 0
for k in range(K):
    Cond, Ques, Ans = GenInsts(Attributes)
    E_c, E_q = InstsEncoder(Cond, Ques)
    AnsRelatedEmbs = CMFF(E_q, E_c, E_I)
    AnsPred = AnswerHead(AnsRelatedEmbs)
    LossSum += AnswerLoss(AnsPred, Ans)
LossSum.backward() # back-propagate
update(IGTR) # AdamW

```

instructions are fed into an instruction encoder to generate *condition* and *question* embeddings. Meanwhile, an image encoder extracts the image embedding from image ARTETA. These embeddings are then fed into a cross-modal feature fusion module (CMFF) to absorb answer-related cross-modal features. In the following, the absorbed embeddings are forwarded to a multi-task answer head, which has four heads aligned with the four types of answers, and each head is responsible for one answer type.

Image encoder. On the image side, SVTR-B backbone [5] (with the rectification module and CTC decoder removed) is utilized as the encoder. Given a text image of size $H \times W \times 3$, the visual features ($F_v \in \mathbb{R}^{\frac{H}{8} \times \frac{W}{4} \times D}$) are extracted by SVTR-B [5]. Subsequently, image embeddings ($E_I \in \mathbb{R}^{\frac{HW}{32} \times D}$) are obtained by flattening the height (H) and width (W) of F_v . Here, $D = 384$ represents the dimension of the features.

Instruction encoder. The instruction encoder aims to extract distinct features for each instruction. Since both *condition* and *question-answer* are composed of character attributes, we can use character attributes to describe the instruction. Therefore, unlike previous methods in the natural image domain employ pre-trained text encoders [20], [48] to encode the instruction, which is computationally costly, we devise a lightweight encoder to map the instruction to two embeddings, i.e., *condition*, and *question* embeddings.

We first inspect the compositional elements of the character attributes, which consist of five basic attribute elements, i.e., character, frequency, position, status, and constraint. All are enumerable. Therefore, as depicted in Fig.

3, the instruction encoder consists of five learnable embedding layers. They are character embedding ($CE \in \mathbb{R}^{C \times D}$), frequency embedding ($FE \in \mathbb{R}^{F \times D}$), position embedding ($PE \in \mathbb{R}^{P \times D}$), status embedding ($SE \in \mathbb{R}^{2 \times D}$), and constraint embedding ($ConsE \in \mathbb{R}^{L \times D}$) layers. In these embeddings, C , P , and F signify the size of the character set, the maximum position index, and the maximum character frequency, respectively. We set P , F and L to the same length. For each attribute element, the encoding begins by mapping it to the index in the corresponding set. Then, its embedding is found by looking up the vector at this index in the corresponding embedding layer.

We then calculate the representation of each *condition* and *question* using attribute elements. For those associated with only one attribute element, they are directly represented by the embedding of that element. For instance, “What is the 4-th character?” is described by a 384-d embedding from PE . Note that some *condition* and *question* are related to multiple attribute elements, e.g., ce , cf and pc . Their representations are obtained by summing the embeddings of its constituent elements. As illustrated in Fig. 3, “The 1st character is A” can be written as 1-A, and the embedding is the sum of the corresponding vectors from CE and PE . Moreover, for questions related to cf_{cons} , the embedding is further added with a constraint embedding from $ConsE$. In addition, since character position and frequency questions (see Tab. 1) are both described by the unitary attribute embedding, a position token ($pt \in \mathbb{R}^{1 \times D}$) and a frequency token ($st \in \mathbb{R}^{1 \times D}$) are also defined. They are added to the corresponding unitary attribute embedding for differentiation. As the example, “How many times does A appears?” can be described by an embedding that sums st and the corresponding vector from CE , and “Which character in the image is R?” is characterized by an embedding summed pt from the vector in CE .

With the embeddings above, we generate the partition-level *condition* and *question* embeddings. The former, i.e., $E_c \in \mathbb{R}^{L_c \times D}$, is obtained by concatenating all *condition* embeddings in that partition. While the latter is obtained by grouping the *question* embeddings into four sets according to answer types, i.e., $E_q = [E_{qc}; E_{qf}; E_{qp}; E_{qs}] \in \mathbb{R}^{L_q \times D}$, where E_{qc} corresponds to question set Q_c and the rest similarly defined. L_q and L_c are the number of *Ques* and *Cond*. Although a large number of instructions are sampled given a text instance, the K partitions and the questions in each partition are independent to each other. They thus can be processed in parallel, which enjoys efficient computation with almost no increase in training cast.

Cross-modal feature fusion. Once instructions and images are successfully encoded, effectively fusing them is crucial for multi-modal tasks. A common practice involves treating the instruction embedding as the *Query* and the image embedding as the *Key* and *Value*, performing cross-attention to extract relevant information from the image modality. Since the instruction in Tab. 1 includes *condition* that represents the known fact, and *question* that denotes the asked question. Thus, it is necessary to construct a new module to enable the effective interaction and fusion of these three embeddings.

We devise a dedicated cross-modal feature fusion (CMFF) module to fuse question (E_q), condition (E_c) and image embeddings (E_I). First, with E_c as *Key* and *Value*,

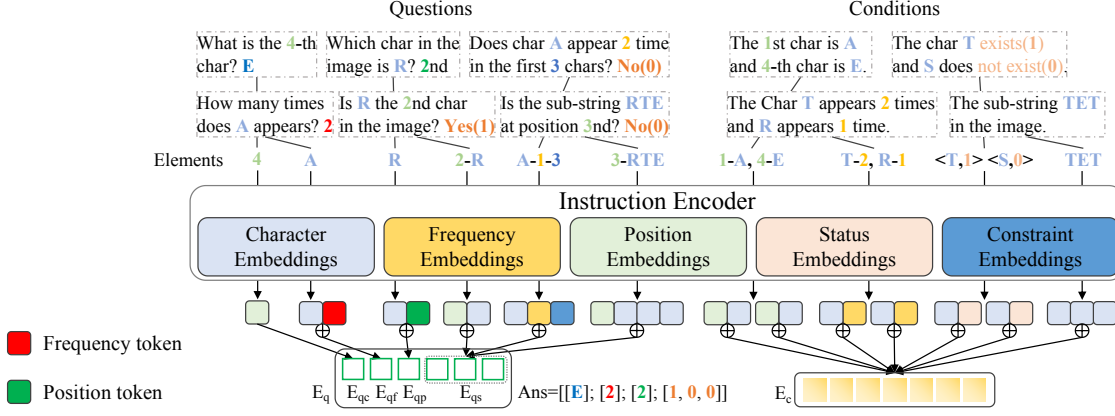


Fig. 3. Details of the instruction encoder. It maps different instructions to feature embeddings by using the five learnable embedding layers placed in the middle of the figure, where different attribute elements or additional tokens are summed to generate a unique *condition* or *question* representation. All *condition* embeddings are concatenated to generate a partition-level representation, and all *question* embeddings are grouped into four classes according to their answer types. Best viewed in color.

and each of the three embedding as *Query*, three multi-head attentions (MHA, Eq. 1) [31] are employed. This process simultaneously performs self-attention on *condition* and cross-attention involving E_c and the other two kinds of embeddings, fully integrating E_c with both other modalities and itself. Second, the same process is performed again with E_I switch E_c as *Key* and *Value*. Consequently, the three modalities further absorb desired information from the image side, effectively enabling IGTR to understand the known attributes and the image content.

$$\begin{aligned} \text{MHA}(Q, K, V) &= [\text{head}_1; \text{head}_2; \dots; \text{head}_h]W^o \\ \text{head}_i &= \text{Attn}_i(VW_i^v) \\ \text{Attn}_i &= \text{softmax}\left(\frac{(QW_i^q)(KW_i^k)^t}{\sqrt{D_h}}\right) \end{aligned} \quad (1)$$

In Eq. 1, there are h attention heads. For the i -th head, it associates with three different weight matrices $W_i^q \in \mathbb{R}^{D \times D_h}$, $W_i^k \in \mathbb{R}^{D \times D_h}$, $W_i^v \in \mathbb{R}^{D \times D_h}$, $[\cdot]$ denotes the concatenation, $D_h = \frac{D}{h}$, and $W^o \in \mathbb{R}^{D \times D}$.

Notably, as shown in the upper right portion of Fig. 2, three MHA modules are involved in each interaction, and their parameters are shared to ensure compact and fast inference of IGTR. In this way, two interactions of the three modalities can be described by Eq. 2:

$$\begin{aligned} \text{Query} &= [E_q; E_c; E_I] \in \mathbb{R}^{(L_q + L_c + \frac{HW}{32}) \times D} \\ \text{Query}^1 &= \text{LN}(\text{MHA}(\text{Query}, E_c, E_c) + \text{Query}) \\ [E_q^1; E_c^1; E_I^1] &= \text{Query}^1 \\ \text{Query}^2 &= \text{LN}(\text{MHA}(\text{Query}^1, E_I^1, E_I^1) + \text{Query}^1) \\ [E_q^2; E_c^2; E_I^2] &= \text{LN}(\text{FFN}(\text{Query}^2) + \text{Query}^2) \end{aligned} \quad (2)$$

where LN means layer normalization.

In the following process (Eq. 3), the E_q^2 from Eq. 2 is employed as *Query*, and question-to-condition and question-to-image cross-attentions are successively conducted, from which the question extracts finer features from both *condi-*

tion and the image domain to obtain answer-related cross-modal embeddings \hat{E}_q .

$$\begin{aligned} E_q^{j1} &= \text{LN}(\text{MHA}(E_q^i, E_c^2, E_c^2) + E_q^j) \\ E_q^{j2} &= \text{LN}(\text{FFN}(E_q^{j1}) + E_q^{j1}) \\ E_q^{j3} &= \text{LN}(\text{MHA}(E_q^{j2}, E_I^2, E_I^2) + E_q^{j2}) \\ E_q^{j+1} &= \text{LN}(\text{FFN}(E_q^{j3}) + E_q^{j3}) \end{aligned} \quad (3)$$

where j starts at 2, E_q^{j*} are the intermediate variables, and E_q^{j+1} denoted as \hat{E}_q is the output of the CMFF.

Multi-task answer head. \hat{E}_q represents the question embedding to be decoded and it can be split into $\hat{E}_{qc} \in \mathbb{R}^{N_c \times D}$, $\hat{E}_{qf} \in \mathbb{R}^{N_f \times D}$, $\hat{E}_{qp} \in \mathbb{R}^{N_p \times D}$, and $\hat{E}_{qs} \in \mathbb{R}^{N_s \times D}$ based on the four answer types. With those embeddings, a multi-task answer head is constructed to perform answer prediction tasks. Specifically, the *character* head, *frequency* head, *status* head, and *position* head are responsible for instructions whose answer is the character, frequency, status (*Yes* or *No*), and position index, respectively. The four heads are all linear classifiers, each associated with learnable parameter matrices: $W_c \in \mathbb{R}^{D \times C}$, $W_f \in \mathbb{R}^{D \times F}$, $W_p \in \mathbb{R}^{D \times 1}$, and $W_s \in \mathbb{R}^{D \times P}$, respectively. Consequently, the prediction answers \hat{A}_c , \hat{A}_f , \hat{A}_p , and \hat{A}_s are obtained applying the four heads to \hat{E}_q :

$$\begin{aligned} \hat{A}_c &= \sigma_1(\hat{E}_{qc}W_c) \in \mathbb{R}^{N_c \times C}, \hat{A}_f = \sigma_1(\hat{E}_{qf}W_f) \in \mathbb{R}^{N_f \times F} \\ \hat{A}_p &= \sigma_1(\hat{E}_{qp}W_p) \in \mathbb{R}^{N_p \times P}, \hat{A}_s = \sigma_2(\hat{E}_{qs}W_s) \in \mathbb{R}^{N_s \times 1} \end{aligned}$$

where N_c , N_f , N_p , and N_s are the number of answers corresponding to the four types, $L_q = N_c + N_f + N_p + N_s$, and σ_1 and σ_2 are softmax and sigmoid functions.

Answer loss. Prediction results of the four heads are compared with the answer label to calculate loss. Assuming \hat{A}_c^n and A_c^n are the prediction and answer label of the n -th question in Q_c and the rest defined similarity, the four losses are calculated as follows and then summed to get a


AR C: None Q: What is 1st char? A: M (✓) C: The 1st char is M . Q: What is 2nd char? A: O (✓) C: The 1st&2nd chars are M&O . Q: What is 3rd char? A: M (✓) C: The 1st, 2nd&3rd chars are M,O&M . Q: What is 4-th char? A: S (✓) C: The 1st, 2nd, 3rd&4-th chars are M,O,M&S . Q: What is 5-th char? A: [E] (✓)		PR C: None Q: What is 1st/2nd/3rd/4-th/5-th... char? A: M (✓) D (✗) M (✓) S (✓) [E] (✓) /... RI C: The 1st, 3rd&4-th chars are M,M&S . Q: What is 2nd char? A: O (✓) ER C: None Q: What is next char of 'sub-string 'MOM'?' A: S (✓) C: None Q: What is next char of 'sub-string 'OMS'?' A: [E] (✓)
---	---	---

Fig. 4. The illustration of different recognition procedures by using different recognition instructions. [E] indicates the end symbol.

Constrained Frequency	Search Status
Q: What are the first chars? A: M Q: How many times does A/.../M/.../O/.../S/... appears in the first 2 chars? A: 0/.../1/.../1/.../0/... Inferring 2nd char is O Q: How many times does A/.../M/.../O/.../S/... appears in the first 3 chars? A: 0/.../2/.../1/.../0/... Inferring 3rd char is M Q: How many times does A/.../M/.../O/.../S/... appears in the first 4 chars? A: 0/.../2/.../1/.../1/... Inferring 4-th char is S End: The text is MOMS.	Q: What are the first chars? A: M Q: Is A/.../M/.../O/.../S/... the 2nd char in the image? A: No/.../No/.../Yes/.../No/... Inferring 2nd char is O Q: Is A/.../M/.../O/.../S/... the 3rd char in the image? A: No/.../Yes/.../No/.../No/... Inferring 3rd char is M Q: Is A/.../M/.../O/.../S/... the 4-th char in the image? A: No/.../No/.../No/.../Yes/... Inferring 4-th char is S End: The text is MOMS.

Fig. 5. Illustration of using the two questions described in Sec. 4.2 for zero-shot text inference of image MOMS. The condition is set to None.

total loss \mathcal{L} according to the Eq. 4:

$$\begin{aligned}
\mathcal{L}_c &= \frac{1}{N_c} \sum_{n=0}^{N_c} \mathcal{L}_{ce}(\hat{A}_c^n, A_c^n, C), \mathcal{L}_f = \frac{1}{N_f} \sum_{n=0}^{N_f} \mathcal{L}_{ce}(\hat{A}_f^n, A_f^n, F) \\
\mathcal{L}_s &= \frac{1}{N_p} \sum_{n=0}^{N_p} \mathcal{L}_{ce}(\hat{A}_p^n, A_p^n, P), \mathcal{L}_p = \frac{1}{N_s} \sum_{n=0}^{N_s} \mathcal{L}_{bce}(\hat{A}_s^n, A_s^n) \\
\mathcal{L} &= \mathcal{L}_c + \mathcal{L}_f + \mathcal{L}_s + \mathcal{L}_p \quad (4)
\end{aligned}$$

where cross-entropy (\mathcal{L}_{ce}) and binary cross-entropy (\mathcal{L}_{bce}) loss are defined as below.

$$\begin{aligned}
\mathcal{L}_{ce}(\hat{Y}, Y, T) &= - \sum_{t=1}^T y_t \log(\hat{y}_t) \\
\mathcal{L}_{bce}(\hat{Y}, Y) &= -y \log(\hat{y}) - (1 - y) \log(1 - \hat{y}) \quad (5)
\end{aligned}$$

3.3 Text Recognition with instruction

When the model is sufficiently trained with character attribute prediction instructions, it is deemed to understand character attributes and the text image. Then, recognition instructions as shown in Tab. 2 are employed for training, where each row corresponds to a different recognition pipeline. Specifically, the first two rows delineate the well-known PR [2], [3] and AR [8], [10] pipelines, standardized in an instruction-guided manner. Similar to existing methods [2], [3], [8], [10], both PR and AR are limited to processing text whose length is up to 25 characters. The third row introduces re-identification (RI). This instruction

TABLE 3
Ablations on instruction variants.

Question (with all conditions)	PR	AR	ER
(a): recognition instructions	80.57	81.27	80.79
(b): (a) + frequency attributes	81.22	82.21	81.98
(c): (b) + position attributes	81.94	83.53	82.18
(d): (c) + sub-string attributes	82.37	84.02	83.21
Condition (with all questions)	PR	AR	ER
(e): w/o condition	79.02	-	-
(f): (e) + cond-1	79.82	-	-
(g): (f) + cond-2	80.90	-	-
(h): (g) + cond-3	81.35	82.93	-
(i): (h) + cond-4	82.23	83.97	83.25
K (with all conditions and questions)	PR	AR	ER
2	80.53	82.41	81.96
4	81.68	83.39	82.85
6	81.92	83.87	83.33
(j): ((d)+constraint, (i)+cond-5, K=8)	82.51	84.86	83.78

can guide the model to double-check the i -th character, which is particularly useful when it is combined with PR or AR to recognize previously misidentified characters. In the fourth row we propose extrapolating recognition (ER), a novel pipeline analogous to AR. Starting from a given sub-string, each time it infers the previous and next characters of the sub-string, thus enabling a sub-string-based stepwisely extending recognition. It offers an elegant way to recognize text whose length is beyond the previous limit of 25 characters. In Fig. 4, we illustrate the recognition procedure by using the four types of instructions, aiding in elucidating their operational principles and implementation nuances.

In addition, benefiting from the flexibility of the instruction-guided paradigm, text recognition can also be achieved by training on character attribute prediction instructions alone (as detailed in Fig. 5), devoid of recognition instructions. Similar to [12]–[14], [20], this pipeline is denoted as *zero-shot* recognition, whose performance we will verify in the experiments.

4 EXPERIMENTS

4.1 Datasets and Implementation Details

We evaluate IGTR on both English and Chinese datasets. For English our models are trained on MJSynth (MJ) [49], [50] and SynthText (ST) [51], two widely used synthetic scene text datasets. Then the models are tested on: (1) six regular and irregular text benchmarks, i.e., ICDAR 2013 (IC13) [52], Street View Text (SVT) [53], IIIT5K-Words (IIIT) [54], ICDAR 2015 (IC15) [55], Street View Text-Perspective (SVTP) [56] and CUTE80 (CUTE) [57]. For IC13 and IC15, we use the versions with 857 and 1,811 images, respectively. We abbreviate the six benchmarks as common benchmarks. (2) Real-world Union14M-L benchmark. It contains over 3.2 million training images and over 0.4 million test images. All are real-world images with both complexity and versatility [58]. The test set includes seven challenging subsets including curve, multi-oriented, artistic, etc. For Chinese, we use Chinese text recognition (CTR) dataset [59], a benchmark containing four subsets: Scene, Web, Document, and Writing. We train the model on the whole training set and use the validation subset of Scene to determine the best model, which is then assessed on the four test subsets.

TABLE 4

Ablations on CMFF components, where recognition accuracy (%) and inference time (ms) are both given.

Model	PR		AR		ER	
	Acc	Time	Acc	Time	Acc	Time
Full Model	82.51	3.98	84.86	10.3	83.78	9.52
(a): w/o Query to Condition	81.75	3.91	82.41	9.87	82.13	9.36
(b): w/o Query to Image	81.85	3.87	82.35	9.54	82.02	9.21
(c): (a) + (b)	80.85	3.77	81.23	9.35	80.83	9.06
(d): w/o Question to Condition	81.96	3.93	82.22	9.86	82.01	9.39
(e): w/o Question to Image	81.34	3.90	83.21	9.53	82.88	9.24
(f): (d) + (e)	80.93	3.81	82.01	9.37	81.25	9.12

We use AdamW optimizer [60] with a weight decay of 0.05 for training. For English models, all images are resized while maintaining their aspect ratio, with a maximum pixel count of 32×128 [11], [34], [61]. The learning rate (LR) is set to 5×10^{-4} and batchsize is set to 768. One cycle LR scheduler [62] with 1.5 epochs linear warm-up is used in all the 20 epochs. The same as [5], [58], [61], data augmentation like rotation, perspective distortion, motion blur and gaussian noise, are randomly performed during training. The alphabet includes all case-insensitive alphanumerics. For Chinese models, all text instances are resized to 32×256 and data augmentation is not performed following [63]. The LR is set to 5×10^{-4} and batchsize is set to 512. One cycle LR scheduler with 3 epochs linear warm-up is used in all 100 epochs. Word accuracy is used as the evaluation metric. The size of the character set C is set to 37 for English and 6625 for Chinese [23]. The maximum prediction length L is set to 25 for both. All models are trained with mixed-precision on 2 Tesla A100 GPUs.

4.2 Ablations

We conduct ablation studies to validate different instruction variants, CMFF components, and model scalability as follows. Note that all models are trained on Union14M-L training set and tested on its test set.

Instruction variants. We conduct experiments to validate the effectiveness of the triplet instructions. The results in Tab. 3 include IGTR-PR (PR), IGTR-AR (AR) and IGTR-ER (ER). In (a), only recognition instructions are utilized for IGTR training. In subsequent variants denoted by (b), (c), (d), and (j), we add questions related to different attributes progressively. For these variants, the attribute prediction instructions are trained first, and then the model is fine-tuned on recognition instructions. The improvements reveal that each attribute contributes positively, supporting that understanding diverse character attributes aids in recognition. Comparing the use of full instructions in (j) to (a), PR improved by +1.94%, AR by +3.59%, and ER by +2.99%, indicating that AR and ER benefit more from the diverse questions, and meanwhile, making use of attributes in *condition* is helpful. On the other hand, we perform (e) with all questions but without condition (*cond*), and then progressively add a condition mode in (f)-(j), where the suffix is the condition index in Tab. 1. IGTR enables AR and ER capabilities only when *cond-3* and *cond-4* are successively added. The results show that *condition* not only enhances accuracy but also realizes different recognition pipelines conveniently by adapting the instructions. Additionally, by

TABLE 5

Ablations on training data volume and model size.

Epoch	20	40	60	Model Size	24M	40M
Vanilla PR	76.14	76.89	77.05	Vanilla PR	76.14	76.23
IGTR-PR	82.51	84.06	85.29	IGTR-PR	82.51	83.60

TABLE 6

Zero-Shot recognition results of using different questions.

Question	Common	Union14M-L
Constrained frequency	94.43	80.22
Search status	95.31	82.33

increasing K , the number of partitions, the accuracy steadily improved, again providing intuitive confirmation of the importance of instruction richness and diversity.

CMFF components. As shown in Fig. 2, CMFF incorporates four cross-attention stages for inter-modal interaction. We devise variants by removing different stages, and the results are presented in Tab. 4. Removing any stage all results in a decrease in accuracy. Notably, the most significant accuracy drop of 2.81% occurs when both query-to-condition and query-to-image stages are removed, emphasizing the necessity of sufficient feature interaction and fusion before making predictions. In addition, for AR and ER the *condition* is preceding decoded characters while for PR is set to None. It is anticipated that query-to-condition and query-to-image have a more pronounced impact on AR and ER, while PR is relatively less affected. The assumption explains a consistent accuracy degradation of 3.63% for AR and 2.95% for ER. Interestingly, PR also experiences a 1.66% decrease, albeit less severe than AR and ER. This could be attributed to that the query-to-condition and query-to-image stages have encoded ample instruction patterns during training, which are beneficial to all three recognition pipelines. In addition, PR, AR, and ER report inference speeds of 3.98ms, 10.3ms and 9.52ms. The speed differences are in accordance with their recognition pipelines. Meanwhile, they run faster than many previous models following similar recognition pipelines. Notably, as shown in Tab. 4, removing cross-attention stages only triggers minor speed acceleration. The results, in turn, verify that CMFF is quite efficient.

Scalability of IGTR. We conduct ablations on training data volume and model size. Specifically, we select IGTR-PR and vanilla PR, where the latter is trained solely using the PR instruction. The results are presented in the left half of Tab. 5, where different training epochs are considered. We observe a notable accuracy gain of 2.78% when increasing epochs from 20 to 60 for IGTR-PR. This improvement is accompanied by the expansion of training data volume, as IGTR-PR samples attribute prediction instructions individually at each epoch. The trained model benefits from richer instructions. In contrast, the improvement of vanilla PR is 0.91%, solely from more training epochs that generate a slightly better model optimization. The significant improvement gap (2.78% v.s. 0.91%) implies that our instruction-guided training is more flexible and can produce more powerful STR models when necessary. Furthermore, the right half of Tab. 5 shows that the accuracy increases with model size. The 24M and 40M models correspond to using SVTR-B and SVTR-L

TABLE 7
Recognition results of rarely appearing characters on CTR [59].

Model	$Rare_{1-10}$	$Rare_{11-30}$	$Rare_{31-50}$	Avg
IGTR-PD	63.88	84.93	88.79	72.25
IGTR-PD-TS	67.47	86.61	89.86	75.05

TABLE 8
Morphologically similar characters and mis-recognitions on CTR [59]. Take “菜-菜” and 8/5 as the example. It means that without considering TS, “菜” has been recognized as “菜” for 8 times, and the number is reduced to 5 when TS is employed.

Char	菜	x	+	太	干	己
	8/5(菜)	8/4(x)	22/14(+)	20/12(太)	13/11(干)	10/6(己)
Char	入	土	域	日	筒	z
	12/8(人)	4/2(土)	6/3(域)	6/5(日)	6/4(筒)	12/5(2)
Char	金	全	内	于	天	凤
	26/15(全)	16/10(金)	15/8(肉)	13/8(子)	12/5(大)	12/9(凤)
Char	v	东	i	字	自	着
	22/15(y)	7/4(乐)	106/86(l)	9/4(字)	8/5(白)	8/6(看)

[5] as the image encoder, with the remaining architecture keeping the same. We observe a similar large improvement gap (1.09% v.s. 0.09%) between the two methods, suggesting that attribute prediction instructions are the key to increase model performance. However, to fairly compare with other models, here we take SVTR-B as the backbone and IGTR models trained from 20 epochs for further analysis.

4.3 Zero-Shot Recognition

As aforementioned, IGTR can evoke a deep understanding of the text image by training exclusively with attribute prediction instructions. It is observed that text recognition can also be achieved by using certain questions. We term such a pipeline as zero-shot recognition, i.e., IGTR-Zero. Specifically, we use two types of questions to enable text inference. They are *constrained frequency* and *search status*. The quantitative results are given in Tab. 6 and Fig. 5 illustrates the recognition procedures. The former question, by combining with another already learned *edge char* question that tells the first character, enables stepwise inference of the second (by setting the second variable in the question as 2), third, and subsequent characters, thus recognizing the whole text. The recognition process shows certain chain-of-thought capabilities as current large models [21], [72]. However, this inference chain is relatively complex and the model only achieves moderate success on challenging datasets (80.22% on Union14M-L). The latter one, by traversing all characters with all positions, presents a more straightforward and less chain-dependent way to determine the text. It reaches an accuracy of 82.33% on Union14M-L. The results indicate that the text image is well understood by instruction-based attribute learning.

4.4 Rare and Similar Character Recognition

Recognizing rarely appearing and morphologically similar characters are two typical challenges in STR, especially for Chinese. Owing to the flexibility of instruction-guided learning, we devise an elegant scheme to alleviate the two challenges by adjusting the rule of instruction sampling. The

first part is for rare characters. Specifically, we first inspect the CTR dataset [59], characters with less than 50 occurrences in the validation set are treated as rare characters. When a text instance contains a rare character c_r , attributes related to c_r are used to generate question-answer pairs, while other attributes are randomly divided into *condition* and *question-answer* pairs as before. In addition, for rare characters that are not in the input text, five of them are randomly selected and are used to generate questions of *search status*. For example, *Is c_i the j -th character in the image?*, where c_i is one randomly selected rare character. By adjusting the sampling rules as above, rare character attributes receive more attention, and thus learned better.

Then we explain how the rule is adjusted for morphologically similar characters. For a given character, we randomly select three characters, which have been misclassified as other characters, as its morphologically similar characters, or all characters are selected if the misclassified characters are less than three. Then, given a text instance, *search status* questions are constructed. For example, for a similar character pair “大-太”, where the first character is the appeared character and the second is its similar character. The answer would be *Yes* when the question is *Is the i -th character “大”?*, and *No* when the question is *Is the i -th character “太”?*. Morphologically similar characters will be better distinguished with the question-answer pairs above.

We term the adjustments above as targeted strengthening (TS) and devise a model termed IGTR-PR-TS to incorporate them. Results on the CTR dataset [59] are presented in Tab. 7 and Tab. 8. In Tab. 7, rare characters are grouped into three classes according to their occurrences. Compared to the raw IGTR-PR, the accuracy gaps are 3.59%, 1.68%, and 1.07% for characters appearing 1 to 10, 11 to 30, and 31 to 50 times, respectively. Larger gains are observed for severely rare characters. Meanwhile in Tab. 8, each character pair gives two values, e.g., 8/5 for the “菜-菜” pair. It means that IGTR-PR classifies “菜” as “菜” 8 times, and the times is reduced from 8 to 5 when IGTR-PR-TS is employed. As can be seen, recognition errors occurred between morphologically similar characters are largely reduced. Both experiments convincingly verify the flexibility of IGTR and its potential to address typical STR challenges.

4.5 Comparison with State-of-the-Art

We then compare IGTR with previous STR models on both Common and Union14M-L [58] benchmarks. The results trained based on synthetic and Union14M-L datasets are presented in Tab. 9 and Tab. 10, respectively. Meanwhile, we also train IGTR in another manner: first pre-training with attribute prediction instructions on synthetic datasets [49]–[51], and then fine-tuning with recognition instructions on Union14M-L. The obtained models are marked with a suffix PT, e.g., IGTR-PR-PT and IGTR-AR-PT.

We first inspect the results trained based on synthetic datasets. As shown in Tab. 9, in *Ours* we give results of four IGTR models corresponding to the four recognition pipelines. Note that IGTR-PR-RI means RI is further incorporated into the PR pipeline. IGTR-AR ranks the top among 11 of the 13 evaluated subsets from both Common and Union14M-L benchmarks. It surpasses IGTR-PR by

TABLE 9

Results on English benchmarks tested against existing models when trained on synthetic datasets. * represents that the result is evaluated on Union14M-L benchmarks using the model they released.

Method	Common Benchmarks							Union14M-L Benchmark								Parameters ($\times 10^6$)	
	IC13	SVT	IIIT	IC15	SVTP	CUTE	Avg	Curve	Multi-Oriented	Artistic	Contextless	Salient	Multi-Words	General	Avg		
CTC	CRNN [1]	91.1	81.6	82.9	69.4	70.0	65.5	76.75	7.5	0.9	20.7	25.6	13.9	25.6	32.0	18.03	8.3
	SVTR-B* [5]	97.1	91.5	96.0	85.2	89.9	91.7	91.90	69.8	37.7	47.9	61.4	66.8	44.8	61.0	55.63	24.6
AR	ASTER [8]	90.8	90.0	93.3	74.7	80.2	80.9	84.98	34.0	10.2	27.7	33.0	48.2	27.6	39.8	31.50	27.2
	NRTR [10]	95.8	91.5	90.1	79.4	86.6	80.9	87.38	31.7	4.4	36.6	37.3	30.6	54.9	48.0	34.79	31.7
	SAR [9]	91.0	84.5	91.5	69.2	76.4	83.5	82.68	44.3	7.7	42.6	44.2	44.0	51.2	50.5	40.64	57.7
	RoScanner [32]	94.8	88.1	95.3	77.1	79.5	90.3	87.52	43.6	7.9	41.2	42.6	44.9	46.9	39.5	38.09	48.0
	OpenCCD [64]	92.2	85.9	91.9	-	-	83.9	-	-	-	-	-	-	-	-	-	-
	SGBANet [65]	95.1	89.1	95.4	-	83.1	88.2	-	-	-	-	-	-	-	-	-	-
	PARSeq* [11]	97.0	93.6	97.0	86.5	88.9	92.2	92.53	63.9	16.7	52.5	54.3	68.2	55.9	56.9	52.62	23.8
	CornerTrans* [66]	97.8	94.6	95.9	86.5	91.5	92.0	93.05	62.9	18.6	56.1	58.5	68.6	59.7	61.0	55.07	86.0
	LevOCR* [67]	96.7	94.4	96.6	86.5	88.8	90.6	92.27	52.8	10.7	44.8	51.9	61.3	54.0	58.1	47.66	109
	SIGA* [68]	97.8	95.1	96.6	86.6	90.5	93.1	93.28	59.9	22.3	49.0	50.8	66.4	58.4	56.2	51.85	113
	CCD* [69]	97.0	94.4	97.2	87.6	91.8	93.3	93.55	66.6	24.2	63.9	64.8	74.8	62.4	64.0	60.10	52.0
	LISTER* [70]	97.9	93.8	96.9	87.5	89.6	90.6	92.72	56.5	17.2	52.8	63.5	63.2	59.6	65.4	54.05	49.9
	CDisNet* [34]	97.4	93.5	96.4	86.0	88.7	93.4	92.57	69.3	24.4	49.8	55.6	72.8	64.3	58.5	56.38	65.5
PR	SRN [2]	95.5	91.5	94.8	82.7	85.1	87.8	89.57	63.4	25.3	34.1	28.7	56.5	26.7	46.3	40.14	54.7
	VisionLAN [29]	95.7	91.7	95.8	83.7	86.0	88.5	90.23	57.7	14.2	47.8	48.0	64.0	47.9	52.1	47.39	32.8
	ABINet [61]	97.4	93.5	96.2	86.0	89.3	89.2	91.93	59.5	12.7	43.3	38.3	62.0	50.8	55.6	46.03	36.7
	GTR [71]	96.8	94.1	95.8	84.6	87.9	92.3	91.92	62.3	13.9	50.0	45.1	67.1	53.4	58.5	50.07	42.1
	MGP-STR* [4]	97.3	94.7	96.4	87.2	91.0	90.3	92.82	55.2	14.0	52.8	48.5	65.2	48.8	59.1	49.09	148
	MATRNet [36]	97.9	95.0	96.6	86.6	90.6	93.5	93.37	63.1	13.4	43.8	41.9	66.4	53.2	57.0	48.40	44.2
	LPV-B* [7]	97.6	94.6	97.3	87.5	90.9	94.8	93.78	68.3	21.0	59.6	65.1	76.2	63.6	62.0	59.40	35.1
Ours	IGTR-PR	97.6	95.2	97.6	88.4	91.6	95.5	94.30	76.9	30.6	59.1	63.3	77.8	62.5	66.7	62.40	24.1
	IGTR-AR	98.6	95.7	98.2	88.4	92.4	95.5	94.78	78.4	31.9	61.3	66.5	80.2	69.3	67.9	65.07	24.1
	IGTR-PR-RI	97.7	95.5	97.7	88.5	91.6	95.5	94.43	77.3	31.0	59.6	64.3	78.4	65.9	67.2	63.40	24.1
	IGTR-ER	97.3	94.9	97.2	88.3	91.7	95.1	94.09	78.2	32.0	60.6	59.1	78.2	57.8	67.1	61.84	24.1

0.48% on common benchmarks and 2.67% Union14M-L, respectively, demonstrating the effectiveness of encoding already recognized characters via *condition*, especially on more challenging Union14M-L. For IGTR-PR-RI v.s. IGTR-PR, 1% improvement is observed on Union14M-L, showing that the re-identification can correct misrecognition to some extent. Moreover, all four IGTR models perform better than all existing models in Tab. 9. For example, IGTR-AR outperforms LPV-B [7], one of the most competitive previous models, by 1.0% and 5.67% on Common and Union14M-L benchmarks, respectively. Those results convincingly indicate the superiority of the comprehension-first and recognition-next paradigm.

We then look into the results on real-world benchmarks in Tab. 10. It is seen that much higher accuracy is observed when the models are trained on Union14M-L, highlighting the importance of more realistic training data. Similarly, IGTR models excel all existing models in Tab. 10. IGTR-PR-PT and IGTR-AR-PT, the two models mixed synthetic data-based pre-training and real-world data-based fine-tuning, perform considerably well. IGTR-AR-PT ranks the top among 11 of the 13 evaluated subsets. This can be explained as more training data is involved, and meanwhile, it follows an easy-to-hard learning procedure, i.e., first pre-trains on less challenging synthetic data and then fine-tunes on more difficult real-world data. For IGTR-AR-PT, the accuracy gap to SVTR-B, one of the best previous models in Tab. 10 is prominent 2.62% and 6.74%, respectively. The results again demonstrate the superiority of our instruction-guided learning. When looking back to the zero-shot recognition results, we observe that the results obtained based on the *search status* question (Tab. 6) are approaching even exceed

existing top-performed models, especially on Union14M-L. This implies the effectiveness of the devised character attribute prediction instructions, which already endow the model with comprehensive text understanding. Note that all IGTR models only differ in training details. These models are all with a size of 24.1M, which is highly competitive compared to existing models.

In Tab. 11, we also give the comparisons on Chinese benchmark [59]. IGTR still outperforms existing models by clear margins. When targeted strengthening (TS) is further employed we observe accuracy gains, which come from the better recognition of rarely appearing and morphologically similar characters. In addition, we observe that typical data augmentation is particularly useful for the CTR benchmark. Adding it can further improve the accuracy up to 3.80% for PR and 4.57% for AR. We argue that on the one hand, the image modality is relatively scarce when trained on the instruction-guided paradigm. On the other hand, the CTR dataset is not big enough for Chinese with thousands of character categories. Data augmentation can mitigate the two issues especially for difficult text, resulting in more prominent improvements on challenging subsets such as Scene and Handwriting. To sum, the experiments also validate the superiority of IGTR and its great cross-language generalization ability.

4.6 Qualitative Analyses

To better understand IGTR, we depict some success and failure cases in Fig. 6. Cases (a)-(i) are all IGTR correctly recognized images, which are rather challenging and many previous methods have failed on them. We illustrate case (i) in detail by asking a few questions and presenting

TABLE 10

Results on English benchmarks tested against existing models when trained on real-world Union14M-L dataset. † denotes that the result is obtained by training the model on Union14M-L using the code they released.

Method		Common Benchmarks						Union14M-L Benchmark								Parameters ($\times 10^6$)	
		IC13 SVT	IIIT	IC15	SVTP	CUTE	Avg	Curve	Multi-Oriented	Artistic	Contextless	Salient	Multi-Words	General	Avg		
CTC	CRNN [1]	91.8	83.8	90.8	71.8	70.4	80.9	81.58	19.4	4.5	34.2	44.0	16.7	35.7	60.4	30.70	8.3
	SVTR-B† [5]	97.5	96.4	97.8	89.3	91.0	96.2	94.72	85.4	87.4	68.9	79.5	84.3	79.1	81.8	80.91	24.6
AR	ASTER [8]	92.6	88.9	94.3	77.7	80.5	86.5	86.75	38.4	13.0	41.8	52.9	31.9	49.8	66.7	42.07	27.2
	NRTR [10]	96.9	94.0	96.2	80.9	84.8	92.0	90.80	49.3	40.6	54.3	69.6	42.9	75.5	75.2	58.20	31.7
	SAR [9]	96.0	92.4	96.6	82.0	85.7	92.7	90.90	68.9	56.9	60.6	73.3	60.1	74.6	76.0	67.20	57.7
	RoScanner [32]	95.7	92.4	96.8	86.4	83.9	93.8	91.50	66.2	54.2	61.4	72.7	60.1	74.2	75.7	66.36	48.0
	MAERec [58]	97.6	96.8	98.0	87.1	93.2	97.9	95.10	81.4	71.4	72.0	82.0	78.5	82.4	82.5	78.60	35.7
	LISTER† [70]	97.4	98.1	98.2	89.2	93.5	95.5	95.33	71.6	55.9	68.9	76.4	68.1	80.2	80.9	71.72	49.9
PR	SRN [2]	94.7	89.5	95.5	79.1	83.9	91.3	89.00	49.7	20.0	50.7	61.0	43.9	51.5	62.7	48.50	54.7
	VisionLAN [29]	95.1	91.3	96.3	83.6	85.4	92.4	90.68	70.7	57.2	56.7	63.8	67.6	47.3	74.2	62.50	32.8
	ABINet [61]	97.2	95.7	97.2	87.6	92.1	94.4	94.03	75.0	61.5	65.3	71.1	72.9	59.1	79.4	69.19	36.7
	MATRNet [36]	97.9	96.9	98.2	88.2	94.1	97.9	95.50	80.5	64.7	71.1	74.8	79.4	67.6	77.9	74.60	44.2
	LPV-B† [7]	97.4	97.4	98.9	89.8	93.0	97.2	95.62	82.4	64.6	74.1	81.0	78.8	81.1	82.8	77.83	30.5
Ours	IGTR-PR	97.7	97.7	98.3	89.8	93.7	97.9	95.86	88.1	89.9	74.2	80.3	82.8	79.2	83.0	82.51	24.1
	IGTR-AR	98.1	98.4	98.7	90.5	94.9	98.3	96.48	90.4	91.2	77.0	82.4	84.7	84.0	84.4	84.86	24.1
	IGTR-PR-RI	97.8	97.8	98.3	89.7	93.8	97.9	95.91	88.6	90.0	74.1	80.6	83.2	79.9	83.5	82.86	24.1
	IGTR-ER	98.1	97.8	98.3	90.5	94.0	97.2	95.99	89.4	92.3	76.2	78.9	84.7	80.9	84.0	83.78	24.1
	IGTR-PR-PT	98.6	98.0	99.1	91.7	96.8	99.0	97.20	92.4	92.1	80.7	83.6	87.7	86.9	85.0	86.92	24.1
	IGTR-AR-PT	98.8	98.3	99.2	92.0	96.8	99.0	97.34	93.0	92.9	81.3	83.4	88.6	88.7	85.6	87.65	24.1

TABLE 11

Results on CTR dataset tested against existing models.

Method	Scene	Web	Document	Hand-writing	Avg	Params
						($\times 10^6$)
CRNN [1]	53.4	57.0	96.6	50.8	64.45	12.4
ASTER [8]	61.3	51.7	96.2	37.0	61.55	27.2
MORAN [73]	54.6	31.5	86.1	16.2	47.10	28.5
SAR [9]	59.7	58.0	95.7	36.5	62.48	27.8
SEED [74]	44.7	28.1	91.4	21.0	46.30	36.1
MASTER [75]	62.8	52.1	84.4	26.9	56.55	62.8
ABINet [61]	66.6	63.2	98.2	53.1	70.28	53.1
TransOCR [76]	71.3	64.8	97.1	53.0	71.55	83.9
SVTR-B† [5]	71.7	73.8	98.2	52.2	73.98	26.3
CCR-CLIP [63]	71.3	69.2	98.3	60.3	74.78	62.0
IGTR-PR	73.1	74.8	98.6	52.5	74.75	29.2
IGTR-AR	75.1	76.4	98.7	55.3	76.37	29.2
IGTR-PR-TS	73.5	75.9	98.7	54.5	75.65	29.2
IGTR-AR-TS	75.6	77.0	98.8	57.3	77.17	29.2
IGTR-PR-TS-Aug	79.5	80.0	99.4	58.9	79.45	29.2
IGTR-AR-TS-Aug	82.0	81.7	99.5	63.8	81.74	29.2

the model’s responses, which are all correct. Note that for current STR models, the model itself could not answer these questions without consulting the recognized text. This example shows the merit of our instruction-guided learning. It well understands character attributes thus leads to correct text reasoning. Nevertheless, there also are a few failure cases. For cases (j)-(m), answers to all the asked questions are logically consistent although misrecognized. For example, case (j) has made exactly the same mistake of recognizing the fifth *F* as *P*. Furthermore, cases (k), (l) and (m) correspond to severely blurred, low-contrast, and overexposed text, respectively. They are quite challenging even for humans. However, a majority of characters are still correctly inferred for these examples, demonstrating that our instruction-guided learning has evoked powerful character understanding capability.

In Fig. 7 we give four examples of long text recognition, which is also a typical STR challenge. The results show that IGTR-ER can recognize text exceeding 25 characters. This



Fig. 6. Success and failure cases. All results are obtained with IGTR-AR trained on Union14M-L. The wrong answers are marked in red.

is because IGTR-ER does not encode the absolute position embedding. Therefore it can overcome this character limit. Nevertheless, the right-bottom case indicates that IGTR-ER may trigger the error of repeated recognition if the same sub-string appears multiple times, which constitutes a practical issue to address.

In addition, as shown in the bottom of Fig. 1, attention maps $Attn = \text{Sum}(Attn_1, Attn_2, \dots, Attn_n)$, where $Attn_i$ (Eq. 1) is generated by *Question to Image Attention and*

SHANGHAIZHIWEICENTURYHOTEL		Dongpu Marketing Service Center	
GT: shanghaizhiweicenturyhotel	GT: dongpumarketingservicecenter	GT: shanghaizhiweicenturyhotel	GT: dongpumarketingservicecenter
PR: shanghaizhiweicenturyhotl	PR: dongpumarketingserviceceer	PR: shanghaizhiweicenturyhotl	PR: dongpumarketingserviceceer
AR: shanghaizhiweicentury	AR: dongpumarketingservicece	AR: shanghaizhiweicentury	AR: dongpumarketingservicece
ER: shanghaizhiweicenturyhotel	ER: dongpumarketingservicecenter	ER: shanghaizhiweicenturyhotel	ER: dongpumarketingservicecenter
Mild foam cleanser containing		SHANDANDANCURSINE-NORTHWEST	
GT: mildfoamcleansercontaining	GT: shandandancursinenorthwest	GT: mildfoamcleansercontaining	GT: shandandancursinenorthwest
PR: mildfoamcleansercontai_ing	PR: shandandancursinenorttw_st	PR: mildfoamcleansercontai_ing	PR: shandandancursinenorttw_st
AR: mildfoamcleansercontainin	AR: shandandancursine	AR: mildfoamcleansercontainin	AR: shandandancursine
ER: mildfoamcleansercontaining	ER: shandandandandandandan...	ER: mildfoamcleansercontaining	ER: shandandandandandandan...

Fig. 7. The results of three recognition pipelines for long text. Incorrect predictions are marked in red and missed predictions are denoted as underlined.

FFN in Fig. 2, can provide a qualitative explanation for IGTR’s superior performance. When performing attribute prediction, the attention maps show that IGTR can accurately pinpoint and focus on characters emphasized in the instructions. This implies that IGTR effectively correlates the instructions and the image content through the proposed CFMM module. The image patterns are well understood thus enabling smooth execution of the related tasks. As a contrast, previous methods struggle with recognizing rarely seen text image patterns (as shown in the upper of Fig. 1).

5 CONCLUSION

In this paper, we have presented IGTR, an instruction-guided multi-modal paradigm to build accurate, fast and lightweight STR models. To gain these attractive properties, we have extended existing question-answer instruction to $\langle condition, question, answer \rangle$ triplet, which not only increases diversity and richness of the questions but also allows efficient parallel learning. We have developed lightweight instruction encoder, cross-modal feature fusion module and multi-task answer head. They together contribute to a series of STR models that present leading accuracy on multiple English and Chinese benchmarks. Meanwhile, the size of these models is uniformly 24.1M and they consume 3.98ms-10.3ms on NVIDIA 1080Ti GPU when inferring a text image. Notably, IGTR enjoys the flexibility of instruction sampling, by adjusting the sampling of character attribute prediction and recognition instructions, various IGTR models are constructed with different balances between accuracy and inference speed. Furthermore, a simple and elegant IGTR model is built to better recognize rarely appearing and morphologically similar characters.

This paper has made a meaningful attempt in constructing small and efficient multi-modal models dedicated to a specific task, i.e., STR. There also are many works ahead. One is long text recognition [70]. Long text is prevalent in real-world applications, as current tools may not well separate multiple words in a line and take them as a whole. Our preliminary attempt has observed the problem of repeated recognition when directly using IGTR-ER. How to tackle this problem is worthy of further study. Another more generic and bigger one is *small* OCR foundation model, which is capable of accurately and efficiently processing multiple OCR-related tasks like text recognition, document understanding, etc. Similar efforts have emerged in other domains recently [72], [77]. We argue that this research would benefit a wide of applications related to OCR.

REFERENCES

- [1] B. Shi, X. Bai, and C. Yao, “An end-to-end trainable neural network for image-based sequence recognition and its application to scene text recognition,” *IEEE Trans. Pattern Anal. Mach. Intell.*, vol. 39, no. 11, pp. 2298–2304, 2017.
- [2] D. Yu, X. Li, C. Zhang, T. Liu, J. Han, J. Liu, and E. Ding, “Towards accurate scene text recognition with semantic reasoning networks,” in *CVPR*, 2020, pp. 12 113–12 122.
- [3] S. Fang, H. Xie, Y. Wang, Z. Mao, and Y. Zhang, “Read Like Humans: Autonomous, bidirectional and iterative language modeling for scene text recognition,” in *CVPR*, 2021, pp. 7098–7107.
- [4] P. Wang, C. Da, and C. Yao, “Multi-Granularity Prediction for scene text recognition,” in *ECCV*, 2022, pp. 339–355.
- [5] Y. Du, Z. Chen, C. Jia, X. Yin, T. Zheng, C. Li, Y. Du, and Y. Jiang, “SVTR: Scene text recognition with a single visual model,” in *IJCAI*, 2022, pp. 884–890.
- [6] Y. Du, Z. Chen, C. Jia, X. Yin, C. Li, Y. Du, and Y. Jiang, “Context perception parallel decoder for scene text recognition,” *CoRR*, vol. abs/2307.12270, 2023.
- [7] B. Zhang, H. Xie, Y. Wang, J. Xu, and Y. Zhang, “Linguistic More: Taking a further step toward efficient and accurate scene text recognition,” in *IJCAI*, 2023, pp. 1704–1712.
- [8] B. Shi, M. Yang, X. Wang, P. Lyu, C. Yao, and X. Bai, “ASTER: An attentional scene text recognizer with flexible rectification,” *IEEE Trans. Pattern Anal. Mach. Intell.*, vol. 41, no. 9, pp. 2035–2048, 2019.
- [9] H. Li, P. Wang, C. Shen, and G. Zhang, “Show, attend and read: A simple and strong baseline for irregular text recognition,” in *AAAI*, 2019, pp. 8610–8617.
- [10] F. Sheng, Z. Chen, and B. Xu, “NRTR: A no-recurrence sequence-to-sequence model for scene text recognition,” in *ICDAR*, 2019, pp. 781–786.
- [11] D. Bautista and R. Atienza, “Scene text recognition with permuted autoregressive sequence models,” in *ECCV*, 2022, pp. 178–196.
- [12] L. Li, P. Zhang, H. Zhang, J. Yang, C. Li, Y. Zhong, L. Wang, L. Yuan, L. Zhang, J. Hwang *et al.*, “Grounded language-image pre-training,” in *CVPR*, 2022, pp. 10 965–10 975.
- [13] S. Liu, Z. Zeng, T. Ren, F. Li, H. Zhang, J. Yang, C. Li, J. Yang, H. Su, J. Zhu *et al.*, “Grounding DINO: Marrying dino with grounded pre-training for open-set object detection,” *CoRR*, vol. abs/2303.05499, 2023.
- [14] A. Kirillov, E. Mintun, N. Ravi, H. Mao, C. Rolland, L. Gustafson, T. Xiao, S. Whitehead, A. Berg, W. Lo, P. Dollar, and R. Girshick, “Segment anything,” in *ICCV*, 2023, pp. 4015–4026.
- [15] X. Wang, X. Zhang, Y. Cao, W. Wang, C. Shen, and T. Huang, “SegGPT: Towards segmenting everything in context,” in *ICCV*, 2023, pp. 1130–1140.
- [16] J. Long, E. Shelhamer, and T. Darrell, “Fully convolutional networks for semantic segmentation,” in *CVPR*, 2015, pp. 3431–3440.
- [17] R. Girshick, J. Donahue, T. Darrell, and J. Malik, “Rich feature hierarchies for accurate object detection and semantic segmentation,” in *CVPR*, 2014, pp. 580–587.
- [18] T. Lin, M. Maire, S. J. Belongie, J. Hays, P. Perona, D. Ramanan, P. Dollár, and C. L. Zitnick, “Microsoft COCO: common objects in context,” in *ECCV*, 2014, pp. 740–755.
- [19] O. Russakovsky, J. Deng, H. Su, J. Krause, S. Satheesh, S. Ma, Z. Huang, A. Karpathy, A. Khosla, M. S. Bernstein, A. C. Berg, and L. Fei-Fei, “ImageNet large scale visual recognition challenge,” *Int. J. Comput. Vis.*, vol. 115, no. 3, pp. 211–252, 2015.
- [20] A. Radford, J. Kim, C. Hallacy, A. Ramesh, G. Goh, S. Agarwal, G. Sastry, A. Askell, P. Mishkin, J. Clark, G. Krueger, and I. Sutskever, “Learning transferable visual models from natural language supervision,” in *ICML*, 2021, pp. 8748–8763.
- [21] H. Liu, C. Li, Q. Wu, and Y. J. Lee, “Visual instruction tuning,” in *NeurIPS*, 2023.
- [22] Y. Liu, B. Yang, Q. Liu, Z. Li, Z. Ma, S. Zhang, and X. Bai, “Textmonkey: An ocr-free large multimodal model for understanding document,” *CoRR*, vol. abs/2403.04473, 2024.
- [23] C. Li, W. Liu, R. Guo, X. Yin, K. Jiang, Y. Du, Y. Du, L. Zhu, B. Lai, X. Hu, D. Yu, and Y. Ma, “PP-OCRv3: More attempts for the improvement of ultra lightweight ocr system,” *CoRR*, vol. abs/2206.03001, 2022.
- [24] Z. Li, B. Yang, Q. Liu, Z. Ma, S. Zhang, J. Yang, Y. Sun, Y. Liu, and X. Bai, “Monkey: Image resolution and text label are important things for large multi-modal models,” in *CVPR*, 2024.
- [25] A. Singh, G. Pang, M. Toh, J. Huang, W. Galuba, and T. Hassner, “TextOCR: Towards large-scale end-to-end reasoning for arbitrary-shaped scene text,” in *CVPR*, 2021, pp. 8802–8812.

- [26] W. Hu, X. Cai, J. Hou, S. Yi, and Z. Lin, "GTC: Guided training of ctc towards efficient and accurate scene text recognition," in *AAAI*, 2020, pp. 11 005–11 012.
- [27] A. Graves, S. Fernández, F. Gomez, and J. Schmidhuber, "Connectionist temporal classification: Labelling unsegmented sequence data with recurrent neural networks," in *ICML*, 2006, p. 369–376.
- [28] Z. Qiao, Y. Zhou, J. Wei, W. Wang, Y. Zhang, N. Jiang, H. Wang, and W. Wang, "PIMNet: a parallel, iterative and mimicking network for scene text recognition," in *ACM MM*, 2021, pp. 2046–2055.
- [29] Y. Wang, H. Xie, S. Fang, J. Wang, S. Zhu, and Y. Zhang, "From Two to One: A new scene text recognizer with visual language modeling network," in *ICCV*, 2021, pp. 14 194–14 203.
- [30] J. Lee, S. Park, J. Baek, S. Oh, S. Kim, and H. Lee, "On recognizing texts of arbitrary shapes with 2d self-attention," in *CVPR Workshops*, 2020, pp. 2326–2335.
- [31] A. Vaswani, N. Shazeer, N. Parmar, J. Uszkoreit, L. Jones, A. Gomez, L. Kaiser, and I. Polosukhin, "Attention is all you need," in *NIPS*, 2017, pp. 5998–6008.
- [32] X. Yue, Z. Kuang, C. Lin, H. Sun, and W. Zhang, "RobustScanner: Dynamically enhancing positional clues for robust text recognition," in *ECCV*, 2020, pp. 135–151.
- [33] Z. Wan, M. He, H. Chen, X. Bai, and C. Yao, "TextScanner: Reading characters in order for robust scene text recognition," in *AAAI*, 2020, pp. 12 120–12 127.
- [34] T. Zheng, Z. Chen, S. Fang, H. Xie, and Y.-G. Jiang, "CDistNet: Perceiving multi-domain character distance for robust text recognition," *Int. J. Comput. Vis.*, vol. 132, no. 2, pp. 300–318, 2024.
- [35] M. Bleeker and M. de Rijke, "Bidirectional scene text recognition with a single decoder," in *ECAI*, vol. 325, 2020, pp. 2664–2671.
- [36] B. Na, Y. Kim, and S. Park, "Multi-modal Text Recognition Networks: Interactive enhancements between visual and semantic features," in *ECCV*, 2022, pp. 446–463.
- [37] C. Jia, Y. Yang, Y. Xia, Y. Chen, Z. Parekh, H. Pham, Q. Le, Y. Sung, Z. Li, and T. Duerig, "Scaling up visual and vision-language representation learning with noisy text supervision," in *ICML*, 2021, pp. 4904–4916.
- [38] G. Lv, X. Jiang, Y. Sun, W. Ni, and F. Nian, "VQA-CLPR: Turning a visual question answering model into a chinese license plate recognizer," in *ICIG*, 2023, pp. 348–359.
- [39] C. Lai, Z. Lu, L. Cao, and R. Pang, "Instruction-Following speech recognition," *CoRR*, vol. abs/2309.09843, 2023.
- [40] P. Wang, A. Yang, R. Men, J. Lin, S. Bai, Z. Li, J. Ma, C. Zhou, J. Zhou, and H. Yang, "OFA: Unifying architectures, tasks, and modalities through a simple sequence-to-sequence learning framework," in *ICML*, 2022, pp. 23 318–23 340.
- [41] S. Antol, A. Agrawal, J. Lu, M. Mitchell, D. Batra, C. Zitnick, and D. Parikh, "VQA: Visual question answering," in *ICCV*, 2015, pp. 2425–2433.
- [42] D. Zhang, S. Li, X. Zhang, J. Zhan, P. Wang, Y. Zhou, and X. Qiu, "SpeechGPT: Empowering large language models with intrinsic cross-modal conversational abilities," in *EMNLP (Findings)*, 2023, pp. 15 757–15 773.
- [43] S. Deshmukh, B. Elizalde, R. Singh, and H. Wang, "Pengi: An audio language model for audio tasks," in *NeurIPS*, 2023.
- [44] J. Gu, Z. Han, S. Chen, A. Beirami, B. He, G. Zhang, R. Liao, Y. Qin, V. Tresp, and P. Torr, "A systematic survey of prompt engineering on vision-language foundation models," *arXiv preprint arXiv:2307.12980*, 2023.
- [45] J.-B. Alayrac, J. Donahue, P. Luc, A. Miech, I. Barr, Y. Hasson, K. Lenc, A. Mensch, K. Millican, M. Reynolds *et al.*, "Flamingo: a visual language model for few-shot learning," in *NeurIPS*, 2022.
- [46] D. Zhu, J. Chen, X. Shen, X. Li, and M. Elhoseiny, "Minigpt-4: Enhancing vision-language understanding with advanced large language models," *arXiv preprint arXiv:2304.10592*, 2023.
- [47] T. Zheng, Z. Chen, J. Bai, H. Xie, and Y.-G. Jiang, "Tps++: attention-enhanced thin-plate spline for scene text recognition," in *IJCAI*, 2023, pp. 1777–1785.
- [48] J. Devlin, M. Chang, K. Lee, and K. Toutanova, "BERT: pre-training of deep bidirectional transformers for language understanding," in *NAACL-HLT*, 2019, pp. 4171–4186.
- [49] M. Jaderberg, K. Simonyan, A. Vedaldi, and A. Zisserman, "Synthetic data and artificial neural networks for natural scene text recognition," *CoRR*, vol. abs/1406.2227, 2014.
- [50] M. Jaderberg, K. Simonyan, A. Vedaldi, and A. Zisserman, "Reading text in the wild with convolutional neural networks," *Int. J. Comput. Vis.*, vol. 116, no. 1, pp. 1–20, 2015.
- [51] A. Gupta, A. Vedaldi, and A. Zisserman, "Synthetic data for text localisation in natural images," in *CVPR*, 2016, pp. 2315–2324.
- [52] D. KaratzasAU, F. ShafaitAU, S. UchidaAU, M. IwamuraAU, L. G. i. BigordaAU, S. R. MestreAU, J. MasAU, D. F. MotaAU, J. A. AlmazànAU, and L. P. de las Heras, "ICDAR 2013 robust reading competition," in *ICDAR*, 2013, pp. 1484–1493.
- [53] K. Wang, B. Babenko, and S. Belongie, "End-to-end scene text recognition," in *ICCV*, 2011, pp. 1457–1464.
- [54] A. Mishra, A. Karteek, and C. V. Jawahar, "Scene text recognition using higher order language priors," in *BMVC*, 2012, pp. 1–11.
- [55] D. Karatzas, L. Gomez-Bigorda, A. Nicolaou, S. Ghosh, A. Bagdanov, M. Iwamura, J. Matas, L. Neumann, V. R. Chandrasekhar, S. Lu, F. Shafait, S. Uchida, and E. Valveny, "ICDAR 2015 competition on robust reading," in *ICDAR*, 2015, pp. 1156–1160.
- [56] T. Q. Phan, P. Shivakumara, S. Tian, and C. L. Tan, "Recognizing text with perspective distortion in natural scenes," in *CVPR*, 2013, pp. 569–576.
- [57] R. Anhar, S. Palaiahnakote, C. S. Chan, and C. L. Tan, "A robust arbitrary text detection system for natural scene images," *Expert Syst. Appl.*, vol. 41, no. 18, p. 8027–8048, 2014.
- [58] Q. Jiang, J. Wang, D. Peng, C. Liu, and L. Jin, "Revisiting scene text recognition: A data perspective," in *ICCV*, 2023, pp. 20 486–20 497.
- [59] J. Chen, H. Yu, J. Ma, M. Guan, X. Xu, X. Wang, S. Qu, B. Li, and X. Xue, "Benchmarking chinese text recognition: Datasets, baselines, and an empirical study," *CoRR*, vol. abs/2112.15093, 2021.
- [60] I. Loshchilov and F. Hutter, "Decoupled weight decay regularization," in *ICLR*, 2019.
- [61] S. Fang, Z. Mao, H. Xie, Y. Wang, C. Yan, and Y. Zhang, "ABINet++: Autonomous, bidirectional and iterative language modeling for scene text spotting," *IEEE Trans. Pattern Anal. Mach. Intell.*, vol. 45, no. 6, p. 7123–7141, 2023.
- [62] I. Loshchilov and F. Hutter, "SGDR: stochastic gradient descent with warm restarts," in *ICLR*, 2017.
- [63] H. Yu, X. Wang, B. Li, and X. Xue, "Chinese text recognition with a pre-trained CLIP-Like model through image-ids aligning," in *ICCV*, 2023, pp. 11 909–11 918.
- [64] C. Liu, C. Yang, and X. Yin, "Open-Set text recognition via character-context decoupling," in *CVPR*, 2022, pp. 4523–4532.
- [65] D. Zhong, S. Lyu, P. Shivakumara, B. Yin, J. Wu, U. Pal, and Y. Lu, "SGBANet: Semantic gan and balanced attention network for arbitrarily oriented scene text recognition," in *ECCV*, 2022, pp. 464–480.
- [66] X. Xie, L. Fu, Z. Zhang, Z. Wang, and X. Bai, "Toward Understanding WordArt: Corner-guided transformer for scene text recognition," in *ECCV*, 2022, pp. 303–321.
- [67] C. Da, P. Wang, and C. Yao, "Levenshtein OCR," in *ECCV*, 2022, pp. 322–338.
- [68] T. Guan, C. Gu, J. Tu, X. Yang, Q. Feng, Y. Zhao, and W. Shen, "Self-Supervised implicit glyph attention for text recognition," in *CVPR*, 2023, pp. 15 285–15 294.
- [69] T. Guan, W. Shen, X. Yang, Q. Feng, Z. Jiang, and X. Yang, "Self-Supervised Character-to-Character distillation for text recognition," in *ICCV*, 2023, pp. 19 473–19 484.
- [70] C. Cheng, P. Wang, C. Da, Q. Zheng, and C. Yao, "LISTER: Neighbor decoding for length-insensitive scene text recognition," in *ICCV*, 2023, pp. 19 484–19 494.
- [71] Y. He, C. Chen, J. Zhang, J. Liu, F. He, C. Wang, and B. Du, "Visual semantics allow for textual reasoning better in scene text recognition," in *AAAI*, 2022, pp. 888–896.
- [72] D. Zhu, J. Chen, X. Shen, X. Li, and M. Elhoseiny, "MiniGPT-4: Enhancing vision-language understanding with advanced large language models," *CoRR*, vol. abs/2304.10592, 2023.
- [73] C. Luo, L. Jin, and Z. Sun, "MORAN: A multi-object rectified attention network for scene text recognition," *Pattern Recognit.*, vol. 90, pp. 109–118, 2019.
- [74] Z. Qiao, Y. Zhou, D. Yang, Y. Zhou, and W. Wang, "SEED: Semantics enhanced encoder-decoder framework for scene text recognition," in *CVPR*, 2020, pp. 13 525–13 534.
- [75] N. Lu, W. Yu, X. Qi, Y. Chen, P. Gong, R. Xiao, and X. Bai, "MASTER: Multi-aspect non-local network for scene text recognition," *Pattern Recognit.*, vol. 117, p. 107980, 2021.
- [76] J. Chen, B. Li, and X. Xue, "Scene Text Telescope: Text-focused scene image super-resolution," in *CVPR*, 2021, pp. 12 021–12 030.
- [77] T. Ren, Q. Jiang, S. Liu, Z. Zeng, W. Liu, H. Gao, H. Huang, Z. Ma, X. Jiang, Y. Chen *et al.*, "Grounding DINO 1.5: Advance the "edge" of open-set object detection," *arXiv preprint arXiv:2405.10300*, 2024.